

**Gravitational instabilities of superspinars**

Paolo Pani\*

*Dipartimento di Fisica, Università di Cagliari, and INFN sezione di Cagliari, Cittadella Universitaria 09042 Monserrato, Italy*

Enrico Barausse†

*Maryland Center for Fundamental Physics, Department of Physics, University of Maryland, College Park, Maryland 20742, USA*

Emanuele Berti‡

*Department of Physics and Astronomy, The University of Mississippi, University, Mississippi 38677-1848, USA  
and Theoretical Astrophysics 350-17, California Institute of Technology, Pasadena, California 91125, USA*

Vitor Cardoso§

*Centro Multidisciplinar de Astrofísica - CENTRA, Department de Física, Instituto Superior Técnico, Avenida Rovisco Pais 1,  
1049-001 Lisboa, Portugal**and Department of Physics and Astronomy, The University of Mississippi, University, Mississippi 38677-1848, USA*

(Received 10 June 2010; published 6 August 2010)

Superspinars are ultracompact objects whose mass  $M$  and angular momentum  $J$  violate the Kerr bound ( $cJ/GM^2 > 1$ ). Recent studies analyzed the observable consequences of gravitational lensing and accretion around superspinars in astrophysical scenarios. In this paper we investigate the dynamical stability of superspinars to gravitational perturbations, considering either purely reflecting or perfectly absorbing boundary conditions at the “surface” of the superspinner. We find that these objects are unstable independently of the boundary conditions, and that the instability is strongest for relatively small values of the spin. Also, we give a physical interpretation of the various instabilities that we find. Our results (together with the well-known fact that accretion tends to spin superspinars down) imply that superspinars are very unlikely astrophysical alternatives to black holes.

DOI: [10.1103/PhysRevD.82.044009](https://doi.org/10.1103/PhysRevD.82.044009)

PACS numbers: 04.20.Dw, 04.20.-q, 04.70.-s, 04.70.Bw

**I. INTRODUCTION**

Superspinars are vacuum solutions of the gravitational field equations whose mass  $M$  and angular momentum  $J = aM$  violate the Kerr bound, i.e.,  $a > M$  (here and elsewhere in this paper we use geometrical units:  $G = c = 1$ ). These geometries could result from high-energy corrections to Einstein’s theory of gravity, such as those that would be present in string-inspired models [1]. String-inspired corrections may require a modification of the metric (or some sort of “excision”) in a small region surrounding the curvature singularity at the origin, in such a way as to “dress” the singularity. While stable stars with  $a > M$  are in principle allowed in general relativity,<sup>1</sup>

superspinars have been proposed as an alternative to black holes (BHs), and they are therefore imagined to have a compactness comparable to that of extremal rotating Kerr BHs and to exist in any mass range. Therefore, the observation of rapidly spinning ultracompact objects could potentially reveal or rule out the existence of superspinars.

One argument against the existence of superspinars was put forward in Ref. [7]. There, the authors constructed a toy model for a superspinner by assuming that the external surface of the superspinner can be modeled as a perfect mirror, i.e., that the reflection coefficient  $\mathcal{R} = 1$  for waves incident on the superspinner. In this case superspinars are destabilized by superradiant effects, i.e., by the ergoregion instability first discussed by Friedman, Schutz, and Comins [8,9]. The ergoregion instability occurs on a dynamical time scale, posing a serious challenge to the existence of these objects in nature. However, a perfectly reflecting surface may be an unrealistic assumption. In general we would expect a frequency-dependent reflection coefficient  $\mathcal{R}(\omega)$ , and correspondingly a frequency-dependent transmission coefficient  $\mathcal{T}(\omega) = 1 - \mathcal{R}(\omega)$ . The exact form of  $\mathcal{R}(\omega)$  depends on the specific model, but unfortunately no exact solutions describing four-dimensional superspinars are known.

\*paolo.pani@ca.infn.it

†barausse@umd.edu

‡berti@phy.olemiss.edu

§vitor.cardoso@ist.utl.pt

<sup>1</sup>Typical equations of state usually lead to stars with  $a/M \lesssim 0.7$  [2,3] that can be treated within a slow-rotation approximation [4]. However, stable, differentially rotating polytropic stars with  $a/M \approx 1.1$  can be produced, e.g., with the Whisky code [5,6]. Also, note that the Kerr bound can be easily violated by *non-compact* objects such as the Earth ( $M/R \sim 7 \times 10^{-10}$ ), which has  $J/M^2 \sim 10^3$ .

A different instability was recently discussed by Dotti *et al.* [10,11]. These authors studied perturbations of a Kerr solution with  $a/M > 1$  (i.e., unlike Ref. [7], they considered an actual naked singularity). They cast the linearized perturbation equations in the form of a self-adjoint operator and analyzed the discrete spectrum of this operator, proving the existence of an infinite number of unstable modes [11].

Here we generalize the stability analyses of Refs. [7,11] focusing on a superspinar model obtained by considering the Kerr solution with  $a > M$ . Besides extending the study of Ref. [7], we also impose an alternative (and perhaps more physical) prescription for the external surface of a four-dimensional superspinar. We assume that a perfectly absorbing surface (a “stringy horizon”) is created by high-energy effects at some radius  $r = r_0$ , and we impose that the reflection coefficient  $\mathcal{R}(\omega) \equiv 0$  at that radius. These purely ingoing boundary conditions at  $r = r_0$  are designed to make superspinars as stable as possible against the ergoregion instability of Ref. [7]. This instability occurs because, when the boundary at  $r = r_0$  is purely reflecting, the negative-energy modes which exist in the ergoregion can only leak to spatial infinity by tunneling through a potential barrier. Modes propagating outside the ergoregion have positive energies. This results in the negative energy of the ergoregion modes to decrease indefinitely, so that their amplitude becomes unbound, triggering an instability. By imposing purely ingoing boundary conditions at  $r = r_0$ , we basically allow the negative energy trapped in the ergoregion to “fall down a sink”; this could quench the instability to some extent. A similar quenching occurs for Kerr BHs with  $a \leq M$ , the role of the sink being played by the BH horizon. Clearly, if the reflection coefficient  $0 < \mathcal{R}(\omega) < 1$  the quenching would be less efficient. Therefore, we conjecture that if superspinars are unstable when  $\mathcal{R}(\omega) \equiv 0$ , it should be impossible to stabilize them using any other choice of boundary conditions.

In this paper we analyze the stability of superspinars by imposing either perfectly absorbing ( $\mathcal{R}(\omega) \equiv 0$ ) or perfectly reflecting ( $\mathcal{R}(\omega) \equiv 1$ ) boundary conditions at some arbitrary radius  $r = r_0$ . We find that, quite independently of  $r_0$  and of the chosen boundary conditions, *superspinars are unstable to linearized gravitational perturbations*. For purely ingoing boundary conditions the instability is slightly weaker than in the perfectly reflecting case, but it still occurs on a dynamical time scale  $\tau \sim M$ , i.e.,  $\tau \sim 5 \times 10^{-6}$  s for an object with  $M = M_\odot$  and  $\tau \sim 5$  s for a supermassive object with  $M \sim 10^6 M_\odot$ . We also show that this result is valid for a wide class of theories of gravity. Our findings undermine several claims made in the literature that superspinars might be detected because the shadow they cast due to gravitational lensing [12,13] or their accretion properties [1,14–18] are different from Kerr BHs with  $a < M$ . While this is true, superspinars are plagued by multiple gravitational instabilities, and there-

fore they are unlikely to be astrophysically viable BH candidates.

## II. A SIMPLE MODEL OF SUPERSPINAR IN FOUR DIMENSIONS

Following Gimon and Horava [1], we model a superspinar of mass  $M$  and angular momentum  $J = aM$  by the Kerr geometry

$$ds_{\text{Kerr}}^2 = -\left(1 - \frac{2Mr}{\Sigma}\right)dt^2 + \frac{\Sigma}{\Delta}dr^2 - \frac{4Mr}{\Sigma}a\sin^2\theta d\phi dt + \Sigma d\theta^2 + \left[(r^2 + a^2)\sin^2\theta + \frac{2Mr}{\Sigma}a^2\sin^4\theta\right]d\phi^2, \quad (1)$$

where  $\Sigma = r^2 + a^2\cos^2\theta$  and  $\Delta = r^2 + a^2 - 2Mr$ . Unlike Kerr BHs, superspinars have  $a/M > 1$  and no horizon. Since the domain of interest is  $-\infty < r < +\infty$ , the space-time possesses naked singularities and closed timelike curves in regions where  $g_{\phi\phi} < 0$  (see, e.g., [19]).

We study linear perturbations around the Kerr metric (1). Using the Kinnersley tetrad and Boyer-Lindquist coordinates, it is possible to separate the angular and radial variables [20]. Small perturbations of a spin- $s$  field are then reduced to the radial and angular master equations

$$\Delta^{-s} \frac{d}{dr} \left( \Delta^{s+1} \frac{dR_{lm}}{dr} \right) + \left[ \frac{K^2 - 2is(r-M)K}{\Delta} + 4is\omega r - \lambda \right] R_{lm} = 0, \quad (2)$$

$$\left[ (1-x^2)_s S_{lm,x} \right]_x + \left[ (a\omega x)^2 - 2a\omega s x + s + {}_s A_{lm} - \frac{(m+sx)^2}{1-x^2} \right] {}_s S_{lm} = 0, \quad (3)$$

where  $x \equiv \cos\theta$ ,  $K = (r^2 + a^2)\omega - am$  and the separation constants  $\lambda$  and  ${}_s A_{lm}$  are related by

$$\lambda \equiv {}_s A_{lm} + a^2\omega^2 - 2am\omega. \quad (4)$$

The equations above describe scalar, electromagnetic and gravitational perturbations when  $s = 0, \pm 1, \pm 2$  respectively. The oscillation frequencies of the modes can be found from the canonical form of Eq. (2). Switching to a “tortoise coordinate”  $r_*$  defined by the condition  $dr_*/dr = (r^2 + a^2)/\Delta$ , we get

$$\frac{d^2 Y}{dr_*^2} + VY = 0, \quad (5)$$

where

$$Y = \Delta^{s/2} (r^2 + a^2)^{1/2} R, \\ V = \frac{K^2 - 2is(r-M)K + \Delta(4ir\omega s - \lambda)}{(r^2 + a^2)^2} - G^2 - \frac{dG}{dr_*},$$

and  $G = s(r - M)/(r^2 + a^2) + r\Delta(r^2 + a^2)^{-2}$ . The eigenvalues  ${}_sA_{lm}$  in Eq. (4) can be expanded in a power series in the parameter  $a\omega$  as [21]

$${}_sA_{lm} = \sum_{n=0} f_{slm}^{(n)}(a\omega)^n. \quad (6)$$

The absence of ingoing waves at infinity implies [22]

$$Y \sim r^{-s} e^{i\omega r_*}, \quad r \rightarrow \infty. \quad (7)$$

The boundary conditions at  $r = r_0$  are crucial. Ref. [7] assumed a perfect mirror at  $r = r_0$ , i.e.,  $Y(r_0) = 0$ . If instead we assume the existence of some ‘‘stringy horizon’’ at  $r_0$ , we must impose purely ingoing waves as  $r \rightarrow r_0$ . Since for  $a > M$  the potential  $V$  is regular at any  $r = r_0$  (including also  $r_0/M = 0$ ), we can write

$$V(r) \sim V(r_0) + \mathcal{O}(r - r_0). \quad (8)$$

By expanding Eq. (5) in series around  $r = r_0$ , we find that the general solution is a superposition of ingoing and outgoing waves:

$$Y \sim Ae^{-ikr_*} + Be^{ikr_*} + \mathcal{O}(r_* - r_0)^3, \quad k^2 = V(r_0), \quad (9)$$

where the sign of  $k$  is chosen to recover the well-known boundary condition for a wave function in an extreme Kerr background ( $a \rightarrow M$  and  $r_0 \rightarrow M$ ):  $k = \omega - m\Omega$ , where  $\Omega = 1/(2M)$  is the angular velocity of an extreme Kerr black hole. Purely ingoing boundary conditions at the stringy horizon imply  $B = 0$  in Eq. (9) or, equivalently,

$$\frac{dY}{dr_*} = -ikY, \quad r \rightarrow r_0. \quad (10)$$

This is the condition we impose in our numerical code.

For each  $\omega$ , we integrate Eq. (5) numerically inward, starting at some large radius (typically  $r_\infty = 400M$ ) where we impose the asymptotic behavior (7). Our results are robust to variations of  $r_\infty$  in a reasonable range. We stop the numerical integration at  $r = r_0$ , where the value of the field  $Y(\omega, r_0)$  is extracted. Finally, we repeat the integration for different values of  $\omega$  until the desired boundary condition (either  $Y(\omega, r_0) = 0$  or Eq. (10)) at  $r = r_0$  is satisfied, typically to within an accuracy of  $10^{-10}$ .

In our numerical computations we make use of the series expansion (6), truncated at fourth order. When  $|a\omega| < 1$ , the series expansion is a very good approximation of the exact eigenvalues. However, in some cases (i.e., when  $|a\omega| \gtrsim 1$ ), instead of the series expansion we have used exact numerical values of  ${}_sA_{lm}$  obtained by solving Eq. (3) with the continued fraction method [23].

We focus on the most relevant gravitational perturbations, described by the Teukolsky equation with  $s = 2$ . To compute unstable modes we also make use of the symmetry [23,24]

$$m \rightarrow -m, \quad \omega \rightarrow -\omega^*, \quad {}_sA_{lm} \rightarrow {}_sA_{l-m}^*. \quad (11)$$

In practice, this symmetry means that modes with azimuthal number  $-m$  can be obtained from those with azimuthal number  $m$  by changing the sign of the real part of the frequency. Therefore, we focus on modes with  $\text{Re}[\omega] = \omega_R > 0$  only.

### III. PERFECT MIRROR

#### A. Unstable modes with $l = m = 2$

Let us start by reviewing and extending the results of Ref. [7], which first found that superspinars with a perfectly reflecting surface are unstable due to the ergoregion instability. In the top panel of Fig. 1 we show unstable frequencies for  $s = l = m = 2$  as a function of the spin parameter  $a/M$  for selected values of  $r_0/M$ . We see that the instability (signalled by a positive imaginary part  $\omega_I$  for the frequency) is always strong, i.e., it always occurs on a short time scale  $\tau \equiv 1/\omega_I \sim 10M \sim 5 \times 10^{-5}(M/M_\odot)$  s, at least when  $a \lesssim 2.2M$ . It is interesting to note that the instability is also effective for  $r_0 = M$  and  $a = M + \epsilon$ , i.e., for an object as compact as an extremal Kerr BH with a rotation parameter that only slightly violates the Kerr bound. This is also illustrated in Table I.

From Fig. 1 and Table I, it is clear that when  $r_0 > M$  the imaginary part does not vanish as  $a \rightarrow M$ . This is in agreement with our expectations, since when  $r_0 > r_H$  the ‘‘BH bomb’’ instability [7,25] occurs even when  $a < M$ .

The dependence of the eigenfrequencies on the mirror location is also shown in the bottom panel of Fig. 1 for different values of the spin parameter. The imaginary part of the frequency is positive (i.e., the object is unstable) for a wide range of parameters. For any value of  $a/M$  in the bottom panel of Fig. 1 the instability is strongest when  $r_0/M \sim 1$ , and is effective also in the limit  $r_0/M \ll 1$  (although in this regime high-energy corrections to the background metric could be relevant).

Overall, Fig. 1 shows that the strongest instability occurs roughly when  $a/M \sim 1.1$ . For larger values of the spin the imaginary part decreases and eventually it vanishes (causing the instability to disappear) for a critical value of  $a/M$  which depends on  $r_0$ . At first sight, this result seems in contrast with the superradiant nature of the instability, as one may naively think that the instability should become stronger for large spins.

In Fig. 2 we show that this expectation is not justified by plotting the proper volume of the ergoregion as a function of  $a/M$ . The proper volume can be computed via

$$V = 4\pi \int_{\theta_i}^{\pi/2} d\theta \int_{r_i}^{r_f} dr \sqrt{g_{rr}g_{\theta\theta}g_{\varphi\varphi}}, \quad (12)$$

where we have considered a constant time slice, the metric elements are taken from Eq. (1), we have exploited the reflection symmetry of the Kerr metric, and we have al-

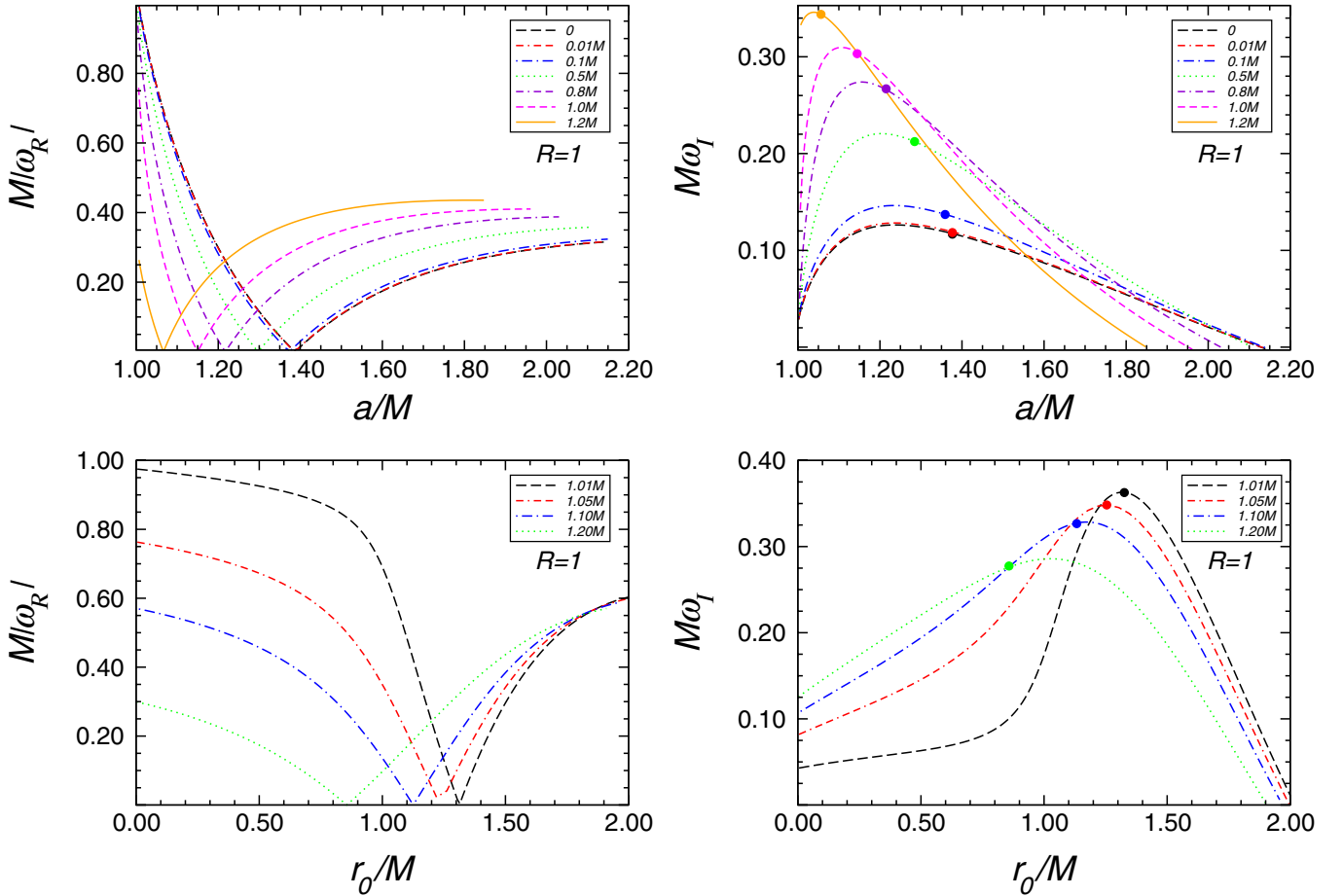


FIG. 1 (color online). Top: Real (left) and imaginary part (right) of unstable gravitational modes of a superspinar as a function of the spin parameter,  $a/M$ , for  $l = m = 2$  and several fixed values of  $r_0$ . Bottom: Real (left) and imaginary part (right) of unstable gravitational modes of a superspinar as a function of the mirror location,  $r_0/M$ , for  $l = m = 2$  and different fixed values of the spin parameter. Large dots indicate purely imaginary modes.

TABLE I. Unstable gravitational ( $s = 2$ ) frequencies with  $l = m = 2$  for a superspinar with a perfect reflecting surface ( $\mathcal{R} = 1$ ) and with a “stringy event horizon” ( $\mathcal{R} = 0$ ) at  $r = r_0$ . All modes in this table have been computed using numerical values of  $s_{A_{lm}}$  obtained via the continued fraction method [23].

$r_0/M$	$(\omega_R M, \omega_I M), \mathcal{R} = 1$			$(\omega_R M, \omega_I M), \mathcal{R} = 0$		
	$a = 1.1M$	$a = 1.01M$	$a = 1.001M$	$a = 1.1M$	$a = 1.01M$	$a = 1.001M$
0.01	(0.5690, 0.1085)	(0.9744, 0.0431)	(0.9810, 0.0097)	(0.5002, 0.0173)	(0.9498, 0.0062)	(1.0286, 0.0033)
0.1	(0.5548, 0.1237)	(0.9673, 0.0475)	(0.9794, 0.0110)	(0.4878, 0.0260)	(0.9435, 0.0093)	(1.0252, 0.0048)
0.5	(0.4571, 0.1941)	(0.9256, 0.0631)	(0.9688, 0.0155)	(0.3959, 0.0719)	(0.9016, 0.0237)	(1.0052, 0.0091)
0.8	(0.3081, 0.2617)	(0.8598, 0.0878)	(0.9507, 0.0202)	(0.2537, 0.1053)	(0.8298, 0.0376)	(0.9793, 0.0095)
1	(0.1364, 0.3095)	(0.6910, 0.1742)	(0.9003, 0.0640)	(0.0916, 0.1219)	(0.6530, 0.0821)	(0.8853, 0.0313)
1.1	(0.0286, 0.3248)	(0.4831, 0.2655)	(0.6071, 0.2207)	(-0.0078, 0.1233)	(0.4377, 0.1230)	(0.5696, 0.1064)

ready integrated out the  $\varphi$  dependence. For  $a < M$  the ergoregion extends between the outer Kerr horizon at  $r_H = M + \sqrt{M^2 - a^2}$  and the “outer ergosphere radius” at  $r_{e+}(\theta) = M + \sqrt{M^2 - a^2 \cos^2 \theta}$ . In this case, we set  $r_i = r_H$ ,  $r_f = r_{e+}$ , and  $\theta_i = 0$  in the integral above. A straightforward calculation shows that in this case the proper volume increases monotonically with  $a/M$ , eventually

diverging<sup>2</sup> for  $a = M$ . However, when  $a > M$ , the ergoregion extends between the inner ergosphere at  $r_{e-}(\theta) = M - \sqrt{M^2 - a^2 \cos^2 \theta}$  and the outer ergosphere  $r_{e+}(\theta)$ .

<sup>2</sup>This is because when  $a = M$ ,  $g_{rr} \sim 1/(r - M)^2$  near the horizon  $r = M$ : this causes the integral (12) to diverge logarithmically.

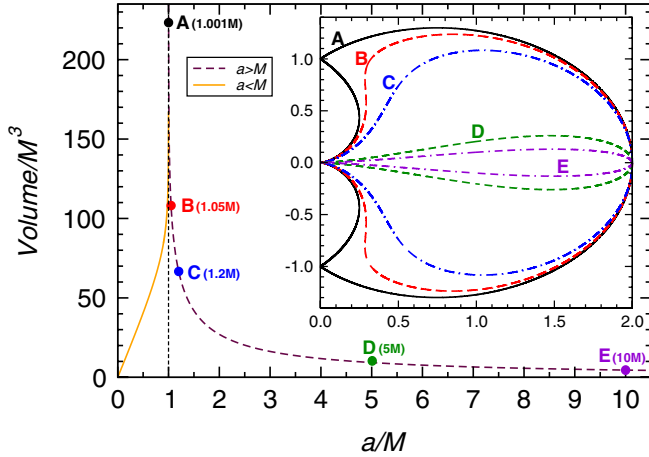


FIG. 2 (color online). Proper volume of the ergoregion as a function of the spin  $a/M$ . The volume increases monotonically when  $a < M$ , is infinite at  $a = M$  and decreases monotonically when  $a > M$ . The proper volumes for  $a \sim 2M$  and  $a \sim 0.3M$  are roughly the same. In the inset we show the azimuthal section of the ergoregion for selected values of the spin. These spins are marked by filled circles and capital Latin letters in the main plot; their numerical value is indicated in parentheses in the figure. In the limit  $a/M \rightarrow \infty$  the ergoregion becomes so oblate that its proper volume shrinks to zero.

Therefore, we set  $r_i = r_{e-}$ ,  $r_f = r_{e+}$ , and  $\theta_i = \arccos(M/a)$  in the integral (12). In this case, the proper volume of the ergosphere monotonically *decreases* with  $a/M$ . In the inset of Fig. 2 we plot an azimuthal section of the ergoregion for selected values of the spin parameter. The proper volume of the ergoregion vanishes as  $a/M \rightarrow \infty$  because the ergoregion becomes more and more oblate (in the equatorial direction) as the spin increases. As  $a/M \rightarrow \infty$  the proper volume shrinks to zero and the ergoregion instability for modes with  $l = m = 2$  becomes

harmless. In Sec. V, however, we will see that this suppression of the ergoregion instability is less effective for modes with  $l = m \gg 2$ , which are more concentrated in the equatorial region and which make superspinners unstable even for larger values of the spin.

### B. Unstable modes with $m = 0$

Superradiance due to an ergoregion is not the only mechanism driving instabilities in superspinners. Unstable modes also exist for  $m = 0$ , when the condition for superradiance  $\omega < m\Omega = 0$  cannot be fulfilled. This is shown in the left panel of Fig. 3, where we show different gravitationally unstable modes for  $l = 2$  and  $m = 0, 1, 2$ .

We see that the unstable mode with  $m = 2$  exists in the range  $0 \leq r_0/M \leq 2$ , i.e., out to the outer location of the ergoregion in the equatorial plane. Unstable modes with  $m = 1$  and  $m = 0$  exist only in a more limited range around  $r_0 \sim M$ . Modes with larger values of  $m (\leq l)$  drive stronger instabilities, but the instability for modes with  $m = 0$  is also important, because it occurs on a dynamical time scale  $\tau = 1/\omega_I \sim M$  for a wide range of parameters. In the right panel of Fig. 3 we show some unstable modes with  $m = 0$  for different values of the spin parameter.

Unstable modes with  $m = 0$  have been recently found by Dotti and Gleiser [10,11]. By imposing regularity conditions at  $r = -\infty$  these authors found (an infinite number of) unstable purely imaginary modes when  $a > M$ . The superspinner model we are discussing reduces to the spacetime considered in Refs. [10,11] when  $r_0 \rightarrow -\infty$  and  $\mathcal{R} = 1$ . We carried out a search of these purely imaginary unstable modes, and our results agree very well with those of Ref. [11] in this limit. For illustration, in the left panel of Fig. 4 we show that the frequency of the  $m = 0$  purely imaginary mode for  $a = 1.4M$  matches the result of Ref. [11] for  $r_0 \rightarrow -\infty$ . The figure shows that the frequency of these modes settles to its asymptotic value

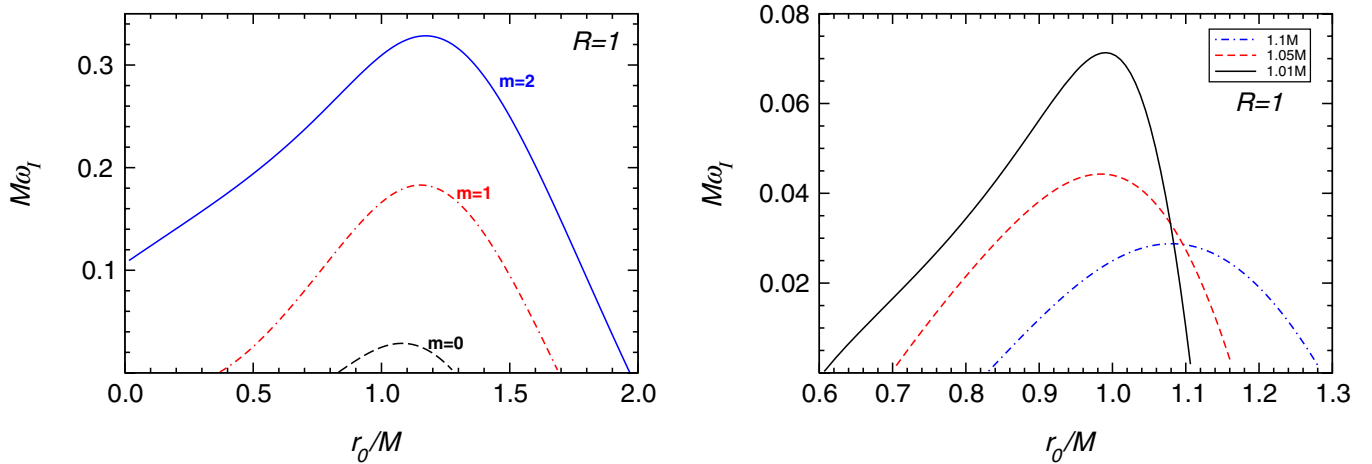


FIG. 3 (color online). Left: Imaginary part of unstable gravitational modes of a superspinner as a function of the mirror location,  $r_0/M$ , for  $a = 1.1M$ ,  $l = 2$  and  $m = 0, 1, 2$ . Right: Imaginary part of unstable gravitational modes of a superspinner as a function of the mirror location,  $r_0/M$ , for  $l = 2$ ,  $m = 0$  and several values of the spin parameter,  $a$ .

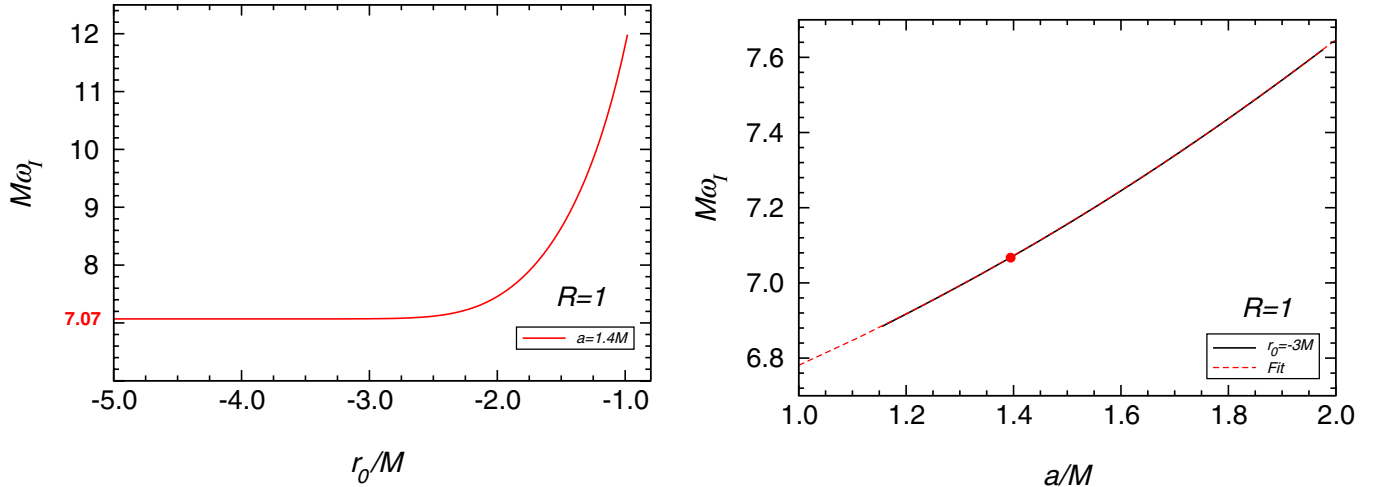


FIG. 4 (color online). Left: Purely imaginary unstable mode as a function of the mirror location,  $r_0/M < 0$ , for  $a = 1.4M$ ,  $s = l = 2$  and  $m = 0$ . In the limit  $r_0 \rightarrow -\infty$ ,  $M\omega_I \sim 7.07$ , which perfectly agrees with results in Ref. [11]. Right: Purely imaginary unstable mode as a function of the spin,  $a/M$ , for  $r_0 = -3M$ ,  $s = l = 2$ ,  $m = 0$ . Numerical results (black straight line) are consistent with the quadratic fit of Eq. (13) (red dashed line). The dot marks the case considered in the left panel.

when  $r_0 \lesssim -3M$ , so it makes sense to fit  $M\omega_I$  for these  $m = 0$  purely imaginary modes as a function of  $a$ , setting  $r_0 = -3M$ . A comparison between the numerical results and the polynomial fit

$$M\omega_I = 6.375 + 0.177a/M + 0.230(a/M)^2 \quad (13)$$

is presented in the right panel of Fig. 4. In the range  $1.15 \lesssim a/M < 2$  the fit is accurate to within 0.003% and suggests that the imaginary part of the frequency (and therefore the “strength” of the instability) grows approximately as a quadratic function of the spin. We stress that these results have been obtained using the asymptotic expansion of the angular spheroidal eigenvalues [21]

$${}_sA_{lm} \sim (2l - \eta + 1)|a\omega| - s(s + 1) + \mathcal{O}(|a\omega|^0), \quad (14)$$

where  $\eta = 2 \max(|m|, |s|)$ . Because for these modes  $|a\omega| \gtrsim 5$ , this expansion is a good approximation of the numerical eigenvalues computed by the continued fraction method [21].

#### IV. ABSORBING BOUNDARY CONDITIONS (HORIZON-LIKE SURFACE AT $r = r_0$ )

From the results discussed in the previous section we conclude that a dynamical instability is almost unavoidable in a broad region of the parameter space if the surface of the superspinar is perfectly reflecting. The instability is present even in what would naively seem the most phenomenologically viable case, i.e., when  $r_0 \sim M$  and  $a = M + \epsilon$ . One could argue that a perfectly reflecting surface maximizes the efficiency of the ergoregion instability because negative-energy modes, which are potentially dangerous, cannot be absorbed, and that this might not happen for different boundary conditions. In fact, Kerr BHs are

stable because (despite superradiant scattering) the negative-energy modes can flow down the horizon. Therefore, we expect ingoing boundary conditions ( $\mathcal{R} = 0$ ) at  $r = r_0$  to represent the worst possible situation for the ergoregion instability to develop. If we find an instability even in this case, the superspinars described by our simple model are doomed to be unstable. This choice also seems more physically motivated than the perfectly reflecting boundary conditions, because  $r_0$  might be the location of an event horizon formed by string-inspired modifications of gravity at high curvatures. We consider both modes with  $l = m = 2$  (which we expect to be affected by the ergoregion instability) as well as modes with  $m = 0$ , which we found to be unstable in the perfectly reflecting case.

The punch line of this section is that unstable modes exist even when we impose ingoing boundary conditions. Qualitatively, the results are the same as those obtained by imposing perfect reflection at the surface of the superspinar. The instability is slightly weaker than in the previous case, but it is again unavoidable in a wide region of parameter space.

Gravitationally unstable modes with  $l = m = 2$  and  $\mathcal{R} = 0$  are listed in Table I and shown in Fig. 5 (to be compared with Fig. 1). Typically the imaginary part of the unstable modes when  $\mathcal{R} = 0$  is only 1 order of magnitude smaller than that obtained imposing  $\mathcal{R} = 1$ , which causes the instability to disappear at slightly smaller spins, i.e., when  $a/M \gtrsim 1.75$ . However, as already mentioned, in the next section we will present evidence that higher- $l$  modes are unstable for larger values of the spin and show that our results are sufficient to rule out superspinars as astrophysically viable alternatives to Kerr BHs.

Also, we stress that perfectly absorbing “stringy horizons” can only be created by high-energy effects taking

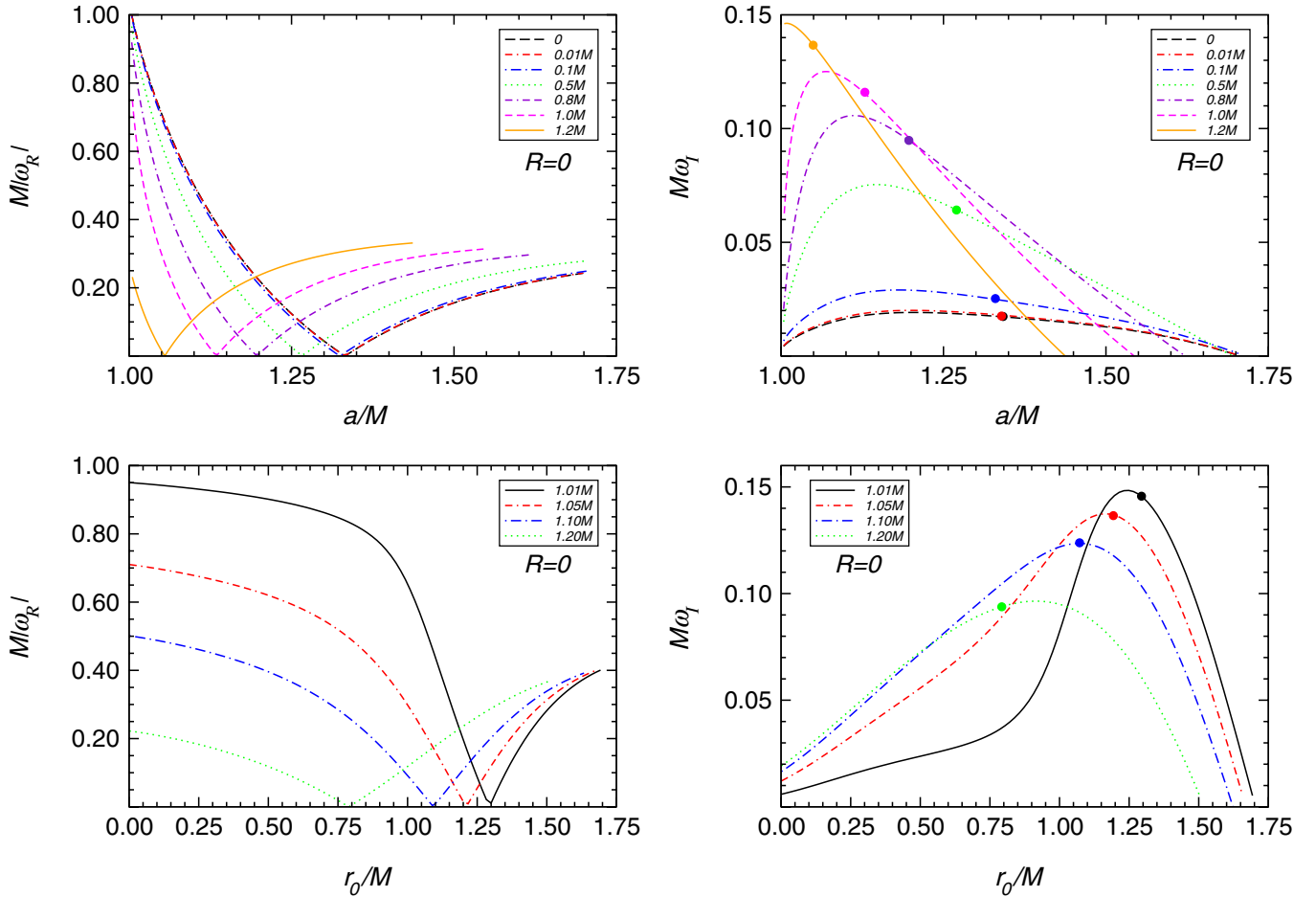


FIG. 5 (color online). Top: Real (left) and imaginary part (right) of unstable gravitational modes of a superspinar as a function of the spin parameter,  $a/M$ , for  $l = m = 2$  and several fixed values of the horizon location  $r_0/M$ . Bottom: Real (left) and imaginary part (right) of unstable gravitational modes of a superspinar as a function of the horizon location, for  $l = m = 2$  and fixed values of the spin parameter. Large dots indicate purely imaginary modes.

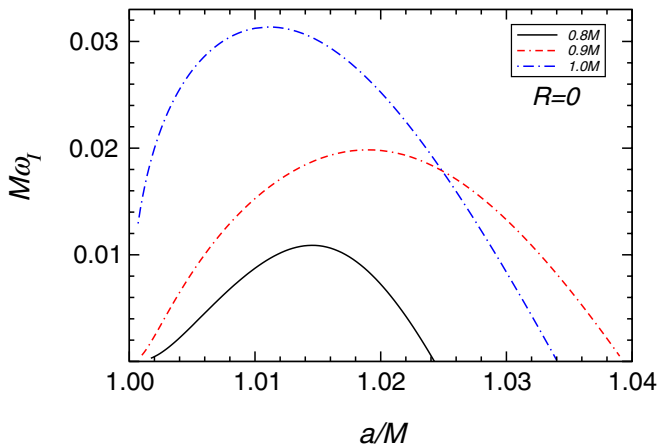


FIG. 6 (color online). Imaginary part of unstable gravitational modes of a superspinar as the spin parameter,  $a$ , for  $l = 2$ ,  $m = 0$  and several values of the horizon location,  $r_0$ .

place beyond the range of validity of general relativity. From a phenomenological point of view, the region that should be modified by these high-energy corrections is close to the curvature singularity of the Kerr metric ( $r_0 \ll M$ ). Unstable modes generically exist for  $a = M + \epsilon$ , even in the limit  $r_0/M \rightarrow 0$ . Moreover, results are smooth in the limit  $r_0/M \rightarrow 0$ , which means that in the region spanned by our calculations curvature singularities do not affect our conclusions.

Finally, Fig. 6 (to be compared with Fig. 3) shows that unstable modes with  $m = 0$  are still present when we impose  $\mathcal{R} = 0$  at  $r = r_0$ .

## V. MODES WITH $l = m \gg 1$ AND PHYSICAL ORIGIN OF THE INSTABILITY

We have seen that when we impose perfectly reflecting boundary conditions ( $\mathcal{R} = 1$ ) superspinars are plagued by several instabilities. Moreover, these instabilities are still present when we impose  $\mathcal{R} = 0$ , i.e., when we consider a

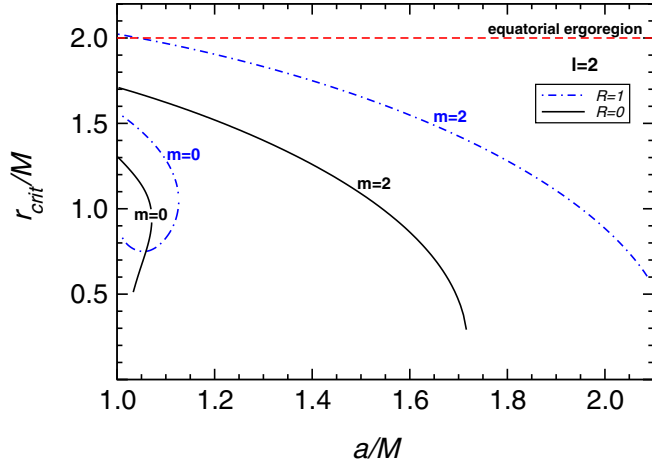


FIG. 7 (color online). Critical radius  $r_{\text{crit}}/M$  as a function of  $a/M$  for  $s = l = 2$  and  $m = 0, 2$ . We impose both  $\mathcal{R} = 0$  and  $\mathcal{R} = 1$  at  $r = r_0$ . For  $m = 2$  an instability occurs when  $r_0 < r_{\text{crit}}$ . For  $m = 0$  an instability occurs in the region delimited by the curves on the left. When  $l = m \gg 1$  an instability is expected to occur also when  $a \geq 2.2M$  in the  $\mathcal{R} = 1$  case, and when  $a \geq 1.75M$  in the  $\mathcal{R} = 0$  case (cf. Figure 8). Although not shown, the region where  $r_0/M < 0$  is expected to be unstable for any value of  $a > M$ .

“stringy horizon” at  $r = r_0$ , which would be expected to quench the instabilities. Here we analyze in more detail how these different instabilities arise. We focus first on the case  $r_0/M > 0$ . For  $\mathcal{R} = 1$  from Figs. 1 and 3 (and analogously for  $\mathcal{R} = 0$  from Figs. 5 and 6) we see that, for both  $m = 0$  and  $m = 2$ , the imaginary part vanishes at some critical radius:  $\omega_I(r_{\text{crit}}) = 0$ . By using a root-finding routine we can solve for the critical radius as a function of the spin parameter  $a/M$ . The results are shown in Fig. 7. For  $m = 2$  and  $\mathcal{R} = 1$  the instability occurs in the region below the dot-dashed blue line extending from  $a \sim M$  up to  $a/M \sim 2.2$ . The dashed horizontal line marks the location of the outer ergoregion on the equatorial plane ( $r = 2M$ ). As  $a/M \rightarrow 1$  the critical radius roughly coincides with the location of the ergoregion, and it decreases monotonically for larger rotation. The situation is similar for  $m = 2$  and  $\mathcal{R} = 0$  (solid black line extending from  $a \sim M$  up to  $a/M \sim 1.75$ ), with the instability disappearing earlier (at  $a/M \sim 1.75$ ) because the ingoing boundary conditions allow negative-energy modes to flow down the stringy horizon. This plot confirms our qualitative understanding of the instability: as shown in Fig. 2, in the limit  $a/M \rightarrow \infty$  the proper volume of the ergoregion vanishes and superradiance cannot destabilize the modes at arbitrarily large spins.

It would therefore seem that superspinars with  $a > 2.2M$  might be stable, for any value of  $r_0$  and even in the most restrictive case with  $\mathcal{R} = 1$ . We argue, however, that this is not true if we consider modes with  $l = m > 2$ . In fact the angular distribution of modes with higher  $l = m$  is more concentrated around the equatorial plane. Higher- $l$  modes

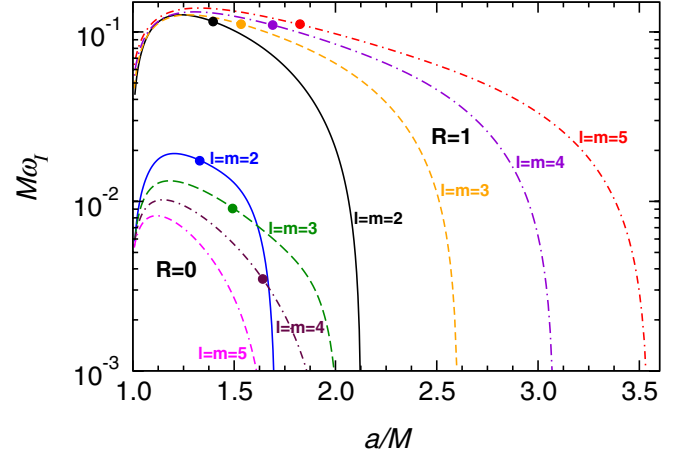


FIG. 8 (color online). Imaginary part of the fundamental unstable mode as a function of the spin  $a/M$  for a superspinner with  $r_0 = 0$ . Upper curves refer to  $\mathcal{R} = 1$  with  $l = m = 2, 3, 4, 5$ . Lower curves refer to  $\mathcal{R} = 0$  with  $l = m = 2, 3, 4, 5$ . Dots indicate purely imaginary modes.

become more effective at destabilizing the superspinner when the ergoregion is oblate, i.e., when  $a \gg M$  (see again the inset of Fig. 2). This intuitive understanding is confirmed by Fig. 8. There we plot the imaginary part of the fundamental unstable modes for  $l = m = 2$  and  $l = m > 2$  (setting  $r_0 = 0$ ), both for  $\mathcal{R} = 1$  and  $\mathcal{R} = 0$ .

In the case  $\mathcal{R} = 1$ , unstable modes with higher  $l = m$  exist for larger values of the spin. For example the  $l = m = 5$  mode becomes stable when  $a/M \geq 3.6$ , while the  $l = m = 2$  mode becomes stable when  $a/M \geq 2.2$ , as previously discussed. Modes with  $l = m \gg 1$  are generally difficult to compute with our code. Our results suggest that, for any fixed value of  $a/M \gg 1$ , there are always unstable modes as long as  $l = m$  is sufficiently large. We stress that these results are in contrast with the case of Kerr BHs, where the superradiant amplification is always stronger for  $l = m = 2$  [22]. Results are qualitatively similar for  $\mathcal{R} = 0$ , in which case the  $l = m = 3$  instability disappears when  $a/M \geq 2$ , while the  $l = m = 2$  instability disappears when  $a/M \geq 1.75$ , as previously discussed. However, in this case the  $l = m = 4$  instability is weaker than the  $l = m = 3$  instability, and the  $l = m = 5$  instability disappears for smaller values of  $a/M$  than in the  $l = m = 2$  case. This is because the stringy event horizon quenches the instability of higher- $l$  modes, similarly to the horizon of a Kerr BH.

More in general, the ergoregion instability that we have found here at the linear level can be related to simple kinematical properties of the Kerr spacetime. In fact, as we show in the Appendix A, Kerr spacetimes with  $a > M$  admit *stable* nonequatorial null circular orbits with *negative* energy. These orbits exist at any radius  $r < M$ . The very existence of these orbits is enough to prove that the spacetime is plagued by the ergoregion instability, *provided* that purely reflecting boundary conditions ( $\mathcal{R} = 1$ )

are imposed at  $r_0 < M$ . This is because null orbits are the geometric-optics limit of gravitational perturbations, as can easily be seen by expanding their propagation equation in powers of  $1/\lambda$  ( $\lambda$  being the wavelength of the perturbation). Therefore, the existence of stable null circular orbits with negative energies implies the existence of short-wavelength modes with negative energies. Under perfectly reflecting boundary conditions, these modes can only leak to infinity by tunneling through the potential barrier. However, because particles outside the ergoregion must have positive energies, this leak makes the energy of the perturbations inside the ergoregion more and more negative. As a result, their amplitude grows without bound, thus revealing the instability of the spacetime. For these reasons we expect modes with  $l = m \gg 1$  to be unstable for arbitrarily large values of  $a/M$ , at least for  $\mathcal{R} = 1$ . This expectation is consistent with the general theorem of Ref. [8], which states that any spacetime possessing an ergoregion, but not an event horizon, is vulnerable to the ergoregion instability. As shown in Fig. 8, this expectation is not always justified in the less efficient case with  $\mathcal{R} = 0$ .

The existence of stable nonequatorial null circular orbits with negative energy clarifies why superspinars are unstable even under perfectly absorbing boundary conditions (i.e., in the presence of a stringy horizon), while for Kerr BHs with  $a \leq M$  the presence of the horizon kills the ergoregion instability. For superspinars, the effective potential for gravitational perturbations presents a minimum at small radii (corresponding, in the eikonal limit, to the location of a negative-energy stable nonequatorial null circular orbit), and then rises as  $r/M \sim 0$ . Therefore, the ergoregion modes need to tunnel through a potential barrier to fall into the “stringy” horizon. The stability of the superspinar depends on a delicate balance between the transmission coefficients through the “inner” and “outer” potential barriers.

A possible objection against instability could be the following. For sufficiently fast rotation (perhaps even for spins as low as  $a \sim 6M$ , i.e., at the higher end of the viable range identified by Ref. [17]), if unstable modes exist in the eikonal limit ( $l = m \rightarrow \infty$ ) their imaginary part will be small, even in the case  $\mathcal{R} = 1$ . The ergoregion instability is due to ergoregion modes leaking to infinity through the potential barrier, but the tunneling becomes less and less effective as the modes behave more and more like particles, because the amplitude transmitted to infinity scales as  $\exp(-L/\lambda)$  (where  $L \sim M$  is the width of the barrier and  $\lambda$  is the mode’s wavelength). It is therefore conceivable that the imaginary part might be so tiny that these modes can be considered stable for all practical purposes.

However, accretion is known to spin superspinars *down* [14]. According to Ref. [26], a BH which is initially non-rotating gets spun up to the extremal limit  $a = M$ , where it cannot be spun up any more [26,27], by accreting a mass  $\Delta M = (\sqrt{6} - 1)M_{\text{in}} = 1.4495M_{\text{in}}$  ( $M_{\text{in}}$  being the initial

BH mass). This corresponds to the accretion of a gas mass  $\Delta M_0 = 1.8464M_{\text{in}}$ , of which  $\Delta M$  falls into the BH and  $\Delta M_0 - \Delta M$  is dissipated by the disk’s viscosity into electromagnetic radiation. Similarly, a superspinar with  $a/M = 7$  gets spun down to  $a/M = 1.5M$  (where the ergoregion instability is always effective) by accreting a mass  $\Delta M = 1.730M_{\text{in}}$  (corresponding to a gas mass  $\Delta M_0 = 2.295M_{\text{in}}$ ). The two processes (spin-up of a Schwarzschild BH to the extremal Kerr limit, and spin-down of a superspinar from  $a/M = 7$  to  $a/M = 1.5$ ) involve amounts of accreted material of the same order of magnitude, hence the corresponding time scales too will be comparable. Supermassive BHs are expected to be spun up to the extremal Kerr limit by coherent accretion<sup>3</sup> on a time scale much smaller than the Hubble time [36], so a superspinar should be spun down to the unstable region on a time scale much smaller than the Hubble time. For this reason, the existence of supermassive superspinars is unlikely in the real Universe.

The situation is slightly different for stellar-mass superspinars. Analytical arguments [37] and population synthesis calculations [38] show that BHs in binaries essentially retain the spin they had at birth, so it is unclear whether accretion would be efficient enough to destabilize a superspinar. On the other hand, as far as we know, no realistic collapse scenario leading to the formation of stellar-mass superspinars has been proposed so far. Typical equations of state lead to compact stars rotating with  $a/M \lesssim 0.7$  [2,3]. Polytropic differentially rotating stars with  $a \approx 1.1M$  can in principle exist [5,6], but they are stable. Even if depleted of 99% of their pressure and induced to collapse, these stars do not form a BH and produce either a supermassive star (which will collapse to a BH with  $a < M$  when enough angular momentum has been shed in gravitational waves) or a stable, rapidly rotating star.

For  $r_0/M > 0$  there is a second family of unstable modes with  $m = 0$  that cannot be superradiant modes. Figures 3 and 6 show that, for fixed values of  $a/M$ , these modes only exist in a limited range of  $r_0/M$ . This range corresponds to the blue dot-dashed line ( $\mathcal{R} = 1$  case) and to the solid black line ( $\mathcal{R} = 0$  case) on the left of Fig. 7, showing that this family of unstable modes only exists for  $a/M \lesssim 1.12$ .

<sup>3</sup>It has been proposed that supermassive BHs may accrete small lumps of material with essentially random orientations of the orbital angular momentum. This “chaotic accretion” results (on average) in a spin-down of the BH [28], so it is very hard to produce fast spinning BHs at all (whereas spin estimates as large as  $a = 0.989^{+0.009}_{-0.002}$  have been reported [29]). Therefore it should be even harder to produce superspinars by chaotic accretion. Binary BH mergers are also known to always produce spins below the Kerr limit [30–35], so one would be left only with the possibility of postulating that supermassive superspinars are born in the early Universe due to high-energy physics effects beyond the realm of classical general relativity.

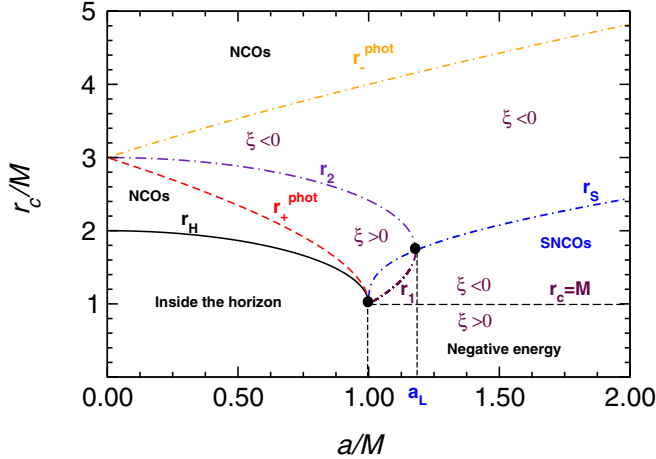


FIG. 9 (color online). The sign of  $\xi = L_z/E$  as a function of  $a/M$  and the radius  $r_c/M$  of null circular orbits. When  $a > M$ ,  $\xi \rightarrow \infty$  at  $r_c = M$ . Stable circular null orbits exist when  $a > M$  for  $r_c < r_s$ , and have negative energy when  $r_c < M$ . Regions marked with NCOs are those where no circular orbits exist. Orbits of constant radius  $r_1$  are stable polar null circular orbits.

These unstable modes are related to the existence of stable “polar” null circular orbits, i.e., circular nonequatorial orbits with vanishing azimuthal component of the orbital angular momentum ( $L_z = 0$ ) [39]. Equation (A22) of the Appendix A (see also Fig. 9) shows that for the Kerr spacetime such orbits exist when  $1 < a/M < (-3 + 2\sqrt{3}) \approx 1.17996$ . For  $l = 4$  and  $\mathcal{R} = 1$  the instability range for modes with  $m = 0$  is  $1 < a/M \lesssim 1.14$ . However, the upper limit of this range is a slowly increasing function of  $l$ , and it is plausible that in the eikonal limit it should tend to  $(-3 + 2\sqrt{3}) \sim 1.18$ .

In conclusion, let us discuss the case  $r_0/M < 0$  (with  $\mathcal{R} = 1$ ), summarized in Fig. 4. Now the ring singularity at  $r/M = 0$  is naked, and the spacetime also possesses closed timelike curves [40]. Therefore it is not surprising that an infinite number of unstable modes exist also at the linear level [11]. At variance with the ergoregion instability, in the present case the imaginary part of the frequency (and therefore the strength of the instability) grows roughly quadratically with  $a/M$  (cf. the right panel of Fig. 4). The same kind of instability has been found in charged, spherically symmetric BHs with naked singularities [10] and therefore it is not related to rotation, but to causality violation (see also the discussion at the end of Ref. [14]). As a matter of fact, we could not find any mode belonging to this family when  $r_0/M \geq 0$ , i.e., when the naked singularity is covered.

In summary, superspinars are plagued by several instabilities for both perfectly reflecting boundary conditions ( $\mathcal{R} = 1$  at  $r = r_0$ ) and perfectly absorbing boundary conditions ( $\mathcal{R} = 0$  at  $r = r_0$ ). The instability of modes with  $l = m$  is related to superradiant scattering. When  $r_0 \sim M$ , unstable modes with  $m = 0$  also exist below some critical

rotation parameter: this instability is related to the existence of stable polar null circular orbits in the spacetime (cf. the Appendix A). Finally, when  $r_0/M < 0$ , a third family of  $m = 0$  modes exists [11]. This third family of unstable modes is probably related to the existence of naked singularity and closed timelike curves in the spacetime.

## VI. CONCLUSIONS

The results reported in this paper indicate that superspinars are unstable independently of the boundary conditions imposed at the “excision radius”  $r_0$  and in a significant region of the two-dimensional parameter space  $(a/M, r_0/M)$ , if not in the whole parameter space. The most effective instability at low rotation rates corresponds to the  $l = m = 2$  (superradiant) mode, but when  $a \sim M$  and  $r_0 \sim M$  unstable modes with  $m = 0$  also exist. The  $l = m = 2$  mode eventually becomes stable at large rotation rates, but unstable modes with  $l = m \gg 1$  are expected to exist for any value of  $a/M$ , at least for  $\mathcal{R} = 1$ . While the instability time scale of higher- $l$  modes may turn out to be very long, making them marginally stable for practical purposes, the low- $l$  instability (which affects superspinars with  $a/M \lesssim 2$ ) takes place on a dynamical time scale. Accretion is known to spin superspinars down [14], so our results indicate that superspinars are unlikely astrophysical alternatives to Kerr BHs.

One possible objection is that, in order to assume incoming boundary conditions at the surface of the superspinner, we must assume that general relativity is modified in that region. Such a modification of general relativity in the excised, high-curvature region surrounding the singularity is implicit in the original superspinner proposal by Gimon and Horava [1], who invoke string theory in order to violate the Kerr bound  $a \leq M$ . We stress, however, that our results hold for a wide class of theories of gravity. Many proposed alternative theories of gravity admit the Kerr spacetime as an exact solution [41,42]. Among these theories, we focus on the large class consisting of Brans-Dicke gravity (with or without a potential), and theories that can be reduced to Brans-Dicke theory with a potential via a conformal transformation (e.g.,  $f(R)$  gravity, both in the metric and Palatini formalism [43,44]). All of these theories admit Kerr-(anti) de Sitter as an exact solution if the scalar field is constant. When perturbed, these solutions satisfy different equations in general relativity and in modified gravity theories [42,45], due to the presence of an extra scalar degree of freedom (the Brans-Dicke scalar), so one might naively expect the stability properties of the Kerr spacetime to be different. However, one can redefine the tensor modes via a conformal transformation so that the vacuum tensor and scalar perturbation equations decouple at linear order [45]. Basically this happens because the Brans-Dicke action reduces to the Einstein-Hilbert action plus a minimally coupled scalar field in the Einstein frame, if no

matter fields are present [44]. Therefore, the tensor modes satisfy the same equations in general relativity as in Brans-Dicke theory (or in any other theory that can be recast in Brans-Dicke form via a conformal transformation.) This means that Eqs. (2) and (3), which are the starting points of our analysis, retain their validity, and therefore that the instability operates in a wider class of gravity theories.

Our results do not imply that there cannot be stable ultracompact objects with  $J/M^2 > 1$ . However, they do imply that either (i) Einstein's gravity should be modified in such a way as to retain Kerr as a solution, while at the same time allowing the tensor modes and the "extra" modes to couple at linear order, or (ii) the structure of astrophysical superspinning objects, if they exist at all, is not described by the simple Kerr-based superspinar proposal of Ref. [1].

### ACKNOWLEDGMENTS

It is a pleasure to thank T. Jacobson for helpful discussions on the problems discussed in this paper, as well as C. Bambi for reading an early version of the manuscript and providing useful comments and suggestions. We also thank S. Dolan for sharing with us some preliminary material on the relation between geodesics and linear perturbations in the Kerr spacetime. E. Barausse acknowledges support from NSF Grant No. PHY-0903631. Emanuele Berti's research was supported by the NSF under Grant No. PHY-0900735. V. Cardoso acknowledges financial support from Fundação Calouste Gulbenkian and from a "Ciência 2007" research contract. This work was partially supported by FCT-Portugal through Project Nos. PTDC/FIS/098025/2008, PTDC/FIS/098032/2008, PTDC/CTE-AST/098034/2008, CERN/FP/109306/2009, and CERN/FP/109290/2009.

### APPENDIX: GEODESICS IN $D$ -DIMENSIONAL KERR SPACETIMES

The main goal of this appendix is to study the existence of stable null circular orbits (SNCOs) with negative energies in Kerr spacetimes. We are interested in these orbits because the very existence of SNCOs (or more generally, the existence of stable null bound orbits) with *negative* energies is enough to show that a spacetime is subject to the ergoregion instability, *provided that* purely reflecting boundary conditions are imposed at the excision surface  $r = r_0$ . For completeness we consider  $D$ -dimensional Kerr spacetimes with only one nonzero angular momentum parameter, and we specialize to the "ordinary"  $D = 4$  case at the end. Our main results for four-dimensional Kerr spacetimes are summarized in Fig. 9. The meaning of the different curves on this plot is explained below.

The metric of a  $D$ -dimensional Kerr BH with only one nonzero angular momentum parameter is given in Boyer-Lindquist-type coordinates by [46]

$$ds^2 = -\frac{\Delta_D - a^2 \sin^2 \vartheta}{\Sigma} dt^2 - \frac{2a(r^2 + a^2 - \Delta_D) \sin^2 \vartheta}{\Sigma} dt d\varphi + \frac{(r^2 + a^2)^2 - \Delta_D a^2 \sin^2 \vartheta}{\Sigma} \sin^2 \vartheta d\varphi^2 + \frac{\Sigma}{\Delta_D} dr^2 + \Sigma d\vartheta^2 + r^2 \cos^2 \vartheta d\Omega_{D-4}^2, \quad (\text{A1})$$

where  $\Sigma = r^2 + a^2 \cos^2 \vartheta$ ,  $\Delta_D = r^2 + a^2 - M_D r^{5-D}$ ,  $d\Omega_{D-4}^2$  denotes the metric of the unit  $(D-4)$  sphere and  $M_D$  and  $a$  are related to the physical mass  $M$  and angular momentum  $J$  of the spacetime

$$M_D = \frac{16\pi M}{D-2} A_D, \quad a = \frac{D-2}{2} \frac{J}{M}, \quad (\text{A2})$$

with  $A_D = (2\pi)^{(1-D)/2} \Gamma[(D-1)/2]$ . The outer horizon is defined as the largest real root of  $r_H^2 + a^2 - M_D r_H^{5-D} = 0$ .

### 1. Equatorial null geodesics

For null geodesics in the equatorial plane ( $\theta = \pi/2$ ) of the spacetime (A1), the radial geodesic equation reads

$$E^{-2} \dot{r}^2 = V_{\text{eff}} = R(r)/r^4 = 1 + \frac{M_D}{r^{D-1}} (\xi - a)^2 - \frac{\xi^2 - a^2}{r^2}, \quad (\text{A3})$$

where  $\xi = L_z/E$  and where the dot denotes derivatives with respect to the dimensionless affine parameter. Conditions for circular orbits are  $V_{\text{eff}}(r_c) = V'_{\text{eff}}(r_c) = 0$ . The condition  $V_{\text{eff}}(r_c) = 0$  implies

$$\xi = \frac{-aM_D \pm \sqrt{r_c^{2(D-3)} \Delta_D(r_c)}}{r_c^{D-3} - M_D} \quad (\text{A4})$$

for direct and retrograde orbits, respectively. For  $D = 4$  the outer horizon is located at  $r = r_H = M + \sqrt{M^2 - a^2}$  and (of course) the Kerr bound implies  $a/M \leq 1$ . The condition  $V'_{\text{eff}}(r_c) = 0$  then leads to three different solutions:

$$r_{\pm}^{\text{phot}} = 2M \left\{ 1 + \cos \left[ \frac{2}{3} \cos^{-1} \left( \mp \frac{a}{M} \right) \right] \right\}, \quad (\text{A5})$$

$$r_{c-} = 2M - \text{Re}[\beta] - \sqrt{3} \text{Im}[\beta],$$

where

$$\beta = [M(-M^2 + 2a^2 + 2a\sqrt{a^2 - M^2})]^{1/3}. \quad (\text{A6})$$

The three solutions are all real. Orbits with  $r_c = r_+^{\text{phot}}$  ( $r_c = r_-^{\text{phot}}$ ) correspond to unstable direct (retrograde) circular orbits lying outside the horizon, whereas  $r_{c-} < r_H$  and therefore this solution does not correspond to physical circular orbits. For  $a > M$ , there is only one real solution

$$r_{\text{phot}} = 2M \left\{ 1 + \cosh \left[ \frac{2}{3} \cosh^{-1} \left( \frac{a}{M} \right) \right] \right\}, \quad (\text{A7})$$

corresponding to an unstable null circular orbit. This is shown in Fig. 9. It is easy to show that the same qualitative results hold also when  $D \geq 5$ . Therefore no stable null equatorial circular orbits exist in  $D$ -dimensional Kerr spacetimes with a single angular momentum parameter.

## 2. Nonequatorial null geodesics

Let us now focus on nonequatorial null geodesics in  $D$ -dimensional Kerr spacetimes with a single spin parameter. We shall follow and generalize the approach discussed in Chandrasekhar's book [47].

The separability of the Hamilton-Jacobi equation in Kerr spacetime was proved by Carter, who also discovered an additional constant of motion  $Q$  (the ‘‘Carter constant’’) besides the energy, the angular momentum and the norm of the four-velocity [40,48]. The same procedure can be easily generalized to  $D$ -dimensional Kerr spacetimes with a single spin parameter, given by Eq. (A1). Our basic equations are

$$\begin{aligned} E^{-2}\Sigma^2\dot{r}^2 &= R(r) \\ &= r^4 + (a^2 - \xi^2 - \eta)r^2 \\ &\quad + M_D[\eta + (\xi - a)^2]r^{5-D} - a^2\eta, \end{aligned} \quad (\text{A8})$$

$$E^{-2}\Sigma^2\dot{\theta}^2 = \Theta(\theta) = \eta + a^2\cos^2\theta - \xi^2\cot^2\theta, \quad (\text{A9})$$

$$\begin{aligned} E^{-1}\Delta_D\Sigma\dot{\phi} &= \Phi(r, \theta) \\ &= \xi\Delta_D\csc^2\theta - a[a\xi + \Delta_D - (r^2 + a^2)], \end{aligned} \quad (\text{A10})$$

$$\begin{aligned} E^{-1}\Delta_D\Sigma\dot{t} &= T(r, \theta) \\ &= (r^2 + a^2)^2 - a^2\Delta_D\sin^2\theta \\ &\quad + a\xi[\Delta_D - (r^2 + a^2)], \end{aligned} \quad (\text{A11})$$

where we use a dot to denote derivatives with respect to the dimensionless affine parameter, and where  $\xi = L_z/E$ ,  $\eta = Q/E$  are two constants of motion. Notice that the angular Eq. (A9) does not depend on  $D$ , and that the equations above reduce to Eqs. (190) and (191) of Ref. [47] when  $D = 4$ .

### A. Proof of no planar bounded orbits in $D$ -dimensional Kerr spacetimes

A relevant question is whether nonequatorial planar orbits exist in these spacetimes. The conditions for a planar orbit ( $\theta = \theta_0 = \text{constant}$ ) are  $\Theta(\theta_0) = 0 = \Theta'(\theta_0)$ . From Eq. (A9) we see that these conditions are fulfilled on the equatorial plane ( $\theta_0 = \pi/2$ ) only if  $\eta = 0$ . For  $\theta_0 \neq \pi/2$  planar orbits exist if

$$\eta = -a^2\cos^4\theta_0, \quad \xi = \pm a\sin^2\theta_0. \quad (\text{A12})$$

For the ‘‘plus’’ branch of the solutions above, the radial Eq. (A8) simply becomes  $\dot{r} = \pm E$ . These geodesics are unbound and describe shear-free null-congruences [47]. The ‘‘minus’’ branch of the solutions describes nonequatorial planar orbits. These solutions only exist when  $D = 4$  and  $a < M$ . Moreover they always lie inside the event horizon, and therefore they do not correspond to physical orbits. For these reasons we do not discuss them further.

## 3. Nonequatorial, circular orbits

Since no planar, nonequatorial circular orbits exist in  $D$ -dimensional Kerr spacetimes, let us focus on nonequatorial, circular orbits, i.e., orbits with constant radius but which are not planar (i.e.,  $\theta$  is not constant). These orbits are periodic [49–51] and they are often called ‘‘spherical orbits’’ in the literature, but here we adopt the term ‘‘circular orbits’’ as in Refs. [49–51].

The conditions for null circular orbits,  $R(r_c) = 0$  and  $R'(r_c) = 0$ , read

$$\begin{aligned} r_c^4 + (a^2 - \xi^2 - \eta)r_c^2 + M_D[\eta + (\xi - a)^2]r_c^{5-D} \\ - a^2\eta = 0, \end{aligned} \quad (\text{A13})$$

$$\begin{aligned} 4r_c^3 + 2(a^2 - \xi^2 - \eta)r_c \\ + (5 - D)M_D[\eta + (\xi - a)^2]r_c^{4-D} = 0, \end{aligned} \quad (\text{A14})$$

which can be solved for  $\xi$  and  $\eta$  as functions of  $r_c$ . There are two sets of solutions:

$$\xi = \frac{r_c^2 + a^2}{a}, \quad \eta = -\frac{r_c^4}{a^2}, \quad (\text{A15})$$

and

$$\begin{aligned} \xi &= \frac{a^2(D-5)M_D r_c^3 + (D-1)M_D r_c^5 - 2r_c^D(a^2 + r_c^2)}{a(D-5)M_D r_c^3 + 2ar_c^D}, \\ \eta &= [a(D-5)M_D r_c^3 + 2ar_c^D]^{-2} \\ &\quad \times \{4M_D r_c^{5+D}(2a^2(D-3) + (D-1)r_c^2) \\ &\quad - (D-1)^2 M_D^2 r_c^{10} - 4r_c^{2(D+2)}\}. \end{aligned} \quad (\text{A16})$$

The first set of solutions implies  $\theta = \text{constant}$  and indeed reduces to the minus branch of solutions (A12), which do not correspond to physical orbits.

The second set of solutions, Eqs. (A16), can describe bound orbits. The condition of stability is simply  $R''(r_c) < 0$ . By differentiating Eq. (A8) twice and using Eqs. (A16) we obtain the following expression for  $R''(r_c)$ :

$$\begin{aligned} R''(r_c) &= [(D-5)M_D r_c^3 + 2r_c^D]^{-2} \\ &\quad \times \{-8(D-5)(D-1)M_D^2 r_c^8 + 32r_c^{2(D+1)} \\ &\quad + 16(D-5)M_D r_c^{D+3}[a^2(D-3) + (D-1)r_c^2]\}. \end{aligned} \quad (\text{A17})$$

The stability of null circular orbits depends on the sign of

the expression above. It is possible to show that stable circular orbits exist for  $D = 4$  and  $a > M$ , but not for  $D \geq 5$ . Therefore in the following we will specialize to  $D = 4$  spacetime dimensions.

### A. $D = 4$ Kerr spacetime

When  $D = 4$ , Eqs. (A16) read

$$\xi = \frac{r_c^2(3M - r_c) - a^2(r_c + M)}{a(r_c - M)}, \quad (\text{A18})$$

$$\eta = \frac{r_c^3[4a^2M - r_c(r_c - 3M)^2]}{a^2(r_c - M)^2}. \quad (\text{A19})$$

These equations correspond to Eqs. (224) and (225) of Ref. [47], and they can be used to define the shadow cast by Kerr BHs or superspinars [12,13]. When  $\eta = 0$ , from Eq. (A19) we have  $4a^2M - r_c(r_c - 3M)^2 = 0$ , which defines the equatorial orbits (A5)–(A7). In general, however, the constant of motion  $\eta$  can be positive or negative. When  $\eta < 0$ , Eqs. (A18) and (A19), together with Eq. (A9) for the  $\theta$ -motion, implies that orbits of constant radius are not allowed [47]. When  $\eta \geq 0$  circular orbits are allowed, and according to Eq. (A19) they must satisfy the condition  $4a^2M - r_c(r_c - 3M)^2 \geq 0$ . For  $a < M$  this condition reads

$$r_+^{\text{phot}} < r_c < r_-^{\text{phot}},$$

where  $r_-^{\text{phot}}$  and  $r_+^{\text{phot}}$  refer to retrograde and direct unstable photon orbits in the equatorial plane [Eq. (A5)]. More importantly for the analysis of superspinars, when  $a > M$  the condition  $\eta > 0$  reads

$$r_c < r_-^{\text{phot}}, \quad (\text{A20})$$

where  $r_-^{\text{phot}}$  is given by Eq. (A7). Notice that the condition above includes also the singular case  $r_c = M$  (in fact  $\xi, \eta \rightarrow \infty$  when  $a > M$  and  $r_c \rightarrow M$ ).

When  $D = 4$ , from Eq. (A17) we see that stable circular orbits exist whenever the orbital radius  $r_c$  satisfies the relation  $r_c < r_S$ , with [12]

$$\frac{r_S}{M} = \begin{cases} 1 + [(a/M)^2 - 1]^{1/3} & \text{for } a > M, \\ 1 - [-(a/M)^2 + 1]^{1/3} & \text{for } a < M. \end{cases} \quad (\text{A21})$$

Null circular orbits with radii smaller than this critical radius are *stable*. When  $a > M$ ,  $r_S < r_-^{\text{phot}}$ , i.e., stable circular orbits are allowed. When  $a < M$  the critical radius  $r_S$  is covered by the horizon, and it becomes “visible” to external observers only when  $a > M$ . Therefore *stable null circular orbits may exist only for  $a > M$* , while orbits with  $r < r_S$  around BHs with  $a < M$  do not have a physical meaning because they lie inside the horizon.

By substituting Eq. (A21) into Eqs. (A18) and (A19) we can compute the corresponding critical parameters  $\eta(r_S) = \eta_S$  and  $\xi(r_S) = \xi_S$ :

$$\frac{\eta_S}{M^2} = \frac{3M^2}{a^2} \left( 1 + \left[ \left( \frac{a}{M} \right)^2 - 1 \right]^{1/3} \right)^4, \\ \frac{\xi_S}{M} = -\frac{a}{M} + \frac{3M}{a} \left( 1 - \left[ \left( \frac{a}{M} \right)^2 - 1 \right]^{2/3} \right).$$

For a given value of  $a/M$ , when  $\eta = \eta_S$  and  $\xi = \xi_S$  we have a marginally stable orbit. If instead  $\xi \approx \xi_S$  we have a stable orbit, while  $\eta \approx \eta_S$  gives a stable orbit if  $a > 3M$  and  $\eta \approx \eta_S$  gives a stable orbit if  $a < 3M$ . However, these are only sufficient conditions, because other stable orbits may exist, far from the critical values  $\eta_S$  and  $\xi_S$ . In fact, depending on the value of the spin we can have different situations: (i) for  $a < 3M$ , if  $\eta < \eta_S(a)$  there is only one stable circular orbit (with  $r_c < M$ ), while for  $\eta > \eta_S(a)$  we have two stable orbits: one with  $r_c < M$  and one with  $r_c > M$ ; (ii) for  $a > 3M$ , when  $\eta < 27M^2$  we have only one stable circular orbit (with  $r_c < M$ ); when  $27M^2 < \eta < \eta_S(a)$  we have two stable orbits with  $r_c > M$  and one with  $r_c < M$ ; when  $\eta > \eta_S(a)$  we have one stable circular orbit with  $r_c < M$  and one with  $r_c > M$ . This can be understood by plotting  $\eta$  as a function of  $r$ , with  $0 < r < r_S(a)$ , for various values of  $a$ .

Also, let us consider the sign of the impact parameter  $\xi = L_z/E$ . A study of Eq. (A18) shows that there is a critical spin

$$a_L = \sqrt{3(-3 + 2\sqrt{3})}M \approx 1.17996M, \quad (\text{A22})$$

such that

- (i) if  $a > a_L$ , then  $\xi > 0$  for  $r_c < M$  and  $\xi < 0$  for  $r_c > M$ . Notice that  $\xi$  diverges if  $r_c = M$ .
- (ii) if  $M < a < a_L$ , then  $\xi > 0$  for  $r_c < M$  and for  $r_1(a) < r_c < r_2(a)$  (with  $r_1, r_2 > M$ ), whereas  $\xi < 0$  elsewhere. Notice that  $\xi$  diverges if  $r_c = M$ .
- (iii) if  $a \leq M$ , then  $\xi > 0$  for  $r_+ < r_c < r_2(a)$ , where  $r_+$  is the outer Kerr horizon and  $r_2 < 3M$ .  $\xi < 0$  for  $r_c > r_2(a)$ .

The situation for a four-dimensional Kerr spacetime is summarized in Fig. 9. Orbits of radius  $r_1$  and  $r_2$  carry vanishing angular momentum ( $L_z = 0$ ) and therefore are called polar null orbits. Orbits of constant radius  $r_2$  are unstable polar null orbits, while orbits of constant radius  $r_1$  are *stable* polar null orbits, and they exist for  $M < a < a_L$ .

A relevant question to ask is whether the null circular orbits that we have identified have positive or negative energy. The sign of the energy is determined by imposing that the geodesics be future oriented, i.e., that the derivative  $i$  of the coordinate time with respect to the affine parameter [given by Eq. (A11)] be positive. (This is because the hypersurfaces  $t = \text{const}$  are spacelike for any  $r > 0$  if  $a > M$ , and for any  $r > r_H$  if  $a \leq M$ .) By substituting Eq. (A18) into Eq. (A11), we find that for the nonequatorial null circular orbits that we have identified we have

$$\dot{t} = \frac{E}{\Sigma} \left[ \frac{r_c^2(r_c + 3M)}{r_c - M} + a^2 \cos^2 \theta \right]. \quad (\text{A23})$$

Because these orbits cross the equatorial plane (as they have  $\eta > 0$ ), we can evaluate Eq. (A23) for  $\theta = \pi/2$ . The energy  $E$  is a constant of motion, so it cannot change sign along the trajectory. Then it is clear that all orbits have  $E > 0$ , with the exception of orbits with  $r_c/M < 1$ , which, as we have seen, exist only for  $a/M > 1$ . Indeed, it is possible to show explicitly that orbits with  $r_c/M < 1$  in Kerr spacetimes with  $a/M > 1$  have negative energy at all times. Using Eq. (A9), one obtains that such orbits have polar angle  $\theta$  oscillating between  $\pi/2 + \theta_c$  and  $\pi/2 - \theta_c$ , with

$$\cos^2 \theta_c = \frac{2r_c \sqrt{M\Delta(a^2M + r_c^2(2r_c - 3M))} - \rho}{a^2(r_c - M)^2}, \quad (\text{A24})$$

where  $\rho = r_c^4 - 3M^2r_c^2 + 2a^2Mr_c$ . One can show that

$\cos^2 \theta_c < 1$  for  $a/M > 1$  and  $r_c/M < 1$ . Using this expression in Eq. (A23) it is then possible to show that the energy must be negative all along trajectories with  $a/M > 1$  and  $r_c/M < 1$ . The region where stable negative-energy orbits exist is shown in Fig. 9.

Finally, let us suppose we have a compact object rotating with  $a > M$ . According to the cosmic censorship conjecture, the singularity at  $r/M = 0$  must be excised by some horizonlike one-way membrane or by a reflecting surface. It is then natural to ask the question of what the compactness of the object can be if one wants to excise all SNCOs with negative energies. Because such orbits exist for any  $r_c < M$ , if  $a > M$ , the maximum allowed compactness turns out to be  $\mu_{\max} = M/r = 1$ . Because orbits with  $r_c \leq M$  lie far away from the singularity at  $r/M = 0$ , this maximum compactness is not expected to be altered by high-energy corrections.

- 
- [1] E. G. Gimon and P. Horava, *Phys. Lett. B* **672**, 299 (2009).
  - [2] G. B. Cook, S. L. Shapiro, and S. A. Teukolsky, *Astrophys. J.* **424**, 823 (1994).
  - [3] E. Berti and N. Stergioulas, *Mon. Not. R. Astron. Soc.* **350**, 1416 (2004).
  - [4] E. Berti, F. White, A. Maniopoulou, and M. Bruni, *Mon. Not. R. Astron. Soc.* **358**, 923 (2005).
  - [5] B. Giacomazzo, L. Rezzolla, and N. Stergioulas (private communication).
  - [6] L. Baiotti, I. Hawke, P. J. Montero, F. Löffler, L. Rezzolla, N. Stergioulas, J. A. Font, and E. Seidel, *Phys. Rev. D* **71**, 024035 (2005).
  - [7] V. Cardoso, P. Pani, M. Cadoni, and M. Cavaglia, *Classical Quantum Gravity* **25**, 195010 (2008).
  - [8] J. L. Friedman, *Commun. Math. Phys.* **63**, 243 (1978).
  - [9] B. F. Schutz and N. Comins, *Mon. Not. R. Astron. Soc.* **182**, 69 (1978).
  - [10] G. Dotti, R. Gleiser, and J. Pullin, *Phys. Lett. B* **644**, 289 (2007).
  - [11] G. Dotti, R. J. Gleiser, I. F. Ranea-Sandoval, and H. Vucetich, *Classical Quantum Gravity* **25**, 245012 (2008).
  - [12] K. Hioki and K.-i. Maeda, *Phys. Rev. D* **80**, 024042 (2009).
  - [13] C. Bambi and N. Yoshida, arXiv:1004.3149.
  - [14] C. Reina and A. Treves, *Astrophys. J.* **227**, 596 (1979).
  - [15] C. Bambi, K. Freese, T. Harada, R. Takahashi, and N. Yoshida, *Phys. Rev. D* **80**, 104023 (2009).
  - [16] C. Bambi, arXiv:0912.4944.
  - [17] R. Takahashi and T. Harada, *Classical Quantum Gravity* **27**, 075003 (2010).
  - [18] C. Bambi, T. Harada, R. Takahashi, and N. Yoshida, *Phys. Rev. D* **81**, 104004 (2010).
  - [19] S. Chandrasekhar, *Proc. R. Soc. A* **392**, 1 (1984).
  - [20] S. A. Teukolsky, *Phys. Rev. Lett.* **29**, 1114 (1972).
  - [21] E. Berti, V. Cardoso, and M. Casals, *Phys. Rev. D* **73**, 024013 (2006).
  - [22] S. A. Teukolsky and W. H. Press, *Astrophys. J.* **193**, 443 (1974).
  - [23] E. Berti, V. Cardoso, and A. O. Starinets, *Classical Quantum Gravity* **26**, 163001 (2009).
  - [24] E. W. Leaver, *Proc. R. Soc. A* **402**, 285 (1985).
  - [25] W. H. Press and S. A. Teukolsky, *Nature (London)* **238**, 211 (1972).
  - [26] J. M. Bardeen, *Nature (London)* **226**, 64 (1970).
  - [27] R. Wald, *Ann. Phys. (N.Y.)* **82**, 548 (1974).
  - [28] A. R. King, J. E. Pringle, and J. A. Hofmann, *Mon. Not. R. Astron. Soc.* **385**, 1621 (2008).
  - [29] L. W. Brenneman and C. S. Reynolds, *Astrophys. J.* **652**, 1028 (2006).
  - [30] U. Sperhake *et al.*, *Phys. Rev. Lett.* **103**, 131102 (2009).
  - [31] E. Berti and M. Volonteri, *Astrophys. J.* **684**, 822 (2008).
  - [32] L. Rezzolla, E. N. Dorband, C. Reisswig, P. Diener, D. Pollney, E. Schnetter, and B. Szilágyi, *Astrophys. J.* **679**, 1422 (2008).
  - [33] L. Rezzolla, E. Barausse, E. N. Dorband, D. Pollney, C. Reisswig, J. Seiler, and S. Husa, *Phys. Rev. D* **78**, 044002 (2008).
  - [34] E. Barausse and L. Rezzolla, *Astrophys. J. Lett.* **704**, L40 (2009).
  - [35] M. Kesden, G. Lockhart, and E. S. Phinney, arXiv:1005.0627.
  - [36] M. Volonteri, P. Madau, E. Quataert, and M. J. Rees, *Astrophys. J.* **620**, 69 (2005).
  - [37] A. R. King and U. Kolb, *Mon. Not. R. Astron. Soc.* **305**, 654 (1999).
  - [38] K. Belczynski, R. E. Taam, E. Rantsiou, and M. van der Sluys, *Astrophys. J.* **682**, 474 (2008).
  - [39] S. Dolan (private communication).
  - [40] B. Carter, *Phys. Rev.* **174**, 1559 (1968).
  - [41] D. Psaltis, D. Perrodin, K. R. Dienes, and I. Mocioiu, *Phys. Rev. Lett.* **100**, 091101 (2008).

- [42] E. Barausse and T.P. Sotiriou, *Phys. Rev. Lett.* **101**, 099001 (2008).
- [43] T.P. Sotiriou and V. Faraoni, *Rev. Mod. Phys.* **82**, 451 (2010).
- [44] D. Wands, *Classical Quantum Gravity* **11**, 269 (1994).
- [45] C.M. Will and H.W. Zaglauer, *Astrophys. J.* **346**, 366 (1989).
- [46] R. C. Myers and M.J. Perry, *Ann. Phys. (N.Y.)* **172**, 304 (1986).
- [47] S. Chandrasekhar, *The Mathematical Theory of Black Holes* (Oxford University Press, New York, 1983).
- [48] B. Carter, *Commun. Math. Phys.* **10**, 280 (1968).
- [49] S. A. Hughes, *Phys. Rev. D* **61**, 084004 (2000); **65**, 069902 (E) (2002)
- [50] S. A. Hughes, *Phys. Rev. D* **64**, 064004 (2001).
- [51] E. Barausse, S. A. Hughes, and L. Rezzolla, *Phys. Rev. D* **76**, 044007 (2007).